

Process Analysis of Ionic Liquid-Based Blends as H₂S Absorbents: Search for Thermodynamic/Kinetic Synergies

Jesús Lemus,* Rubén Santiago, Daniel Hospital-Benito, Tom Welton, Jason P. Hallett, and José Palomar

Cite This: *ACS Sustainable Chem. Eng.* 2021, 9, 2080–2088

Read Online

ACCESS |



Metrics & More



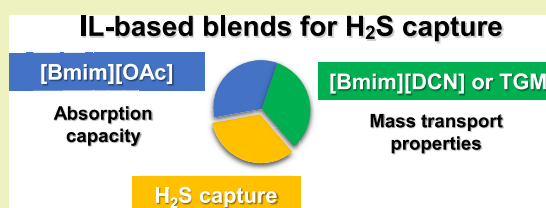
Article Recommendations



Supporting Information

ABSTRACT: Acid gas absorption by ionic liquids (ILs) has arisen as a promising alternative technique for biogas or natural gas upgrading. In the present work, IL-based blends are evaluated for potential thermodynamic/kinetic synergistic effects on hydrogen sulfide (H₂S) capture through physical and/or chemical absorption. First, a molecular simulation analysis by means of COSMO-RS was used to select IL-based blends with enhanced H₂S absorbent thermodynamic properties. Physical absorption parameters of reference (K_{Henry}) for H₂S in several IL-based blends were calculated at 298 K, involving both IL mixtures and conventional industrial absorbents (tetraglyme (TGM)) with ILs at different compositions. A Henry's constant deviation parameter ($\Delta H_{K_{\text{Henry}}}^{\text{H}_2\text{S}}$) was employed to analyze the nonideal effects of the mixture on H₂S gas solubility in IL-based blends. In addition, the viscosities and diffusivities of the IL-based blends were estimated as key parameters controlling H₂S diffusion and absorbent uptake rates. From this analysis, a sample of IL-based blends with promising thermodynamic and kinetic properties was selected for H₂S physical absorption. A process simulation analysis using the COSMO-based/Aspen Plus methodology was then carried out and the selected absorbents were evaluated by modeling H₂S capture in an industrial-scale commercial packed column. One IL, 1-butyl-3-methylimidazolium acetate ([Bmim][OAc]), presenting high H₂S chemical absorption and a low viscous industrial solvent (TGM) were also included. The strong kinetic control of H₂S capture by physical absorption indicated the limited potential performance of IL-based blends or neat ILs in industrial equipment. In contrast, the COSMO/Aspen analysis revealed that adequate formulations based on [Bmim][OAc] and TGM present enhanced H₂S absorbent properties compared to the neat compounds. These computational results may be used to guide future experimental research to design new H₂S absorbents, reducing the highly demanding experimental input.

KEYWORDS: H₂S capture, COSMO-RS, ionic liquid-based blends, absorption, aspen plus



INTRODUCTION

Hydrogen sulfide (H₂S) is a very toxic and corrosive compound appearing in industrial gas and oil process streams.^{1,2} H₂S is heavier than air and therefore tends to linger in poorly ventilated and low-lying areas.² It causes irritation and reacts with water to produce a corrosive acid,³ one of the root causes of acid rain (after oxidizing to SO₂).⁴ Therefore, total H₂S removal from these streams is essential not only for safe transport but also for downstream utilization. Moreover, H₂S elimination improves the calorific value of the natural gas,⁵ so solutions for better H₂S removal are constantly being investigated by the scientific community.

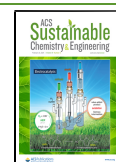
One approach is to employ adsorption operations, using adsorbents such as activated carbon, silica, or zeolites.^{6,7} Highly porous materials such as zeolites have demonstrated high efficiency and high H₂S selectivity and stability even at elevated temperatures.⁸ Nevertheless, the main drawback of this technology is the high energy requirement of the regeneration stage that limits its practical application.⁹ Chemical absorbents such as aqueous solutions of alkanolamines or binary mixtures of monoethanolamine and diethanolamine are used in industries to eliminate H₂S from

natural gas.^{10,11} However, there are also difficulties in the commercial use of these alkanolamine solutions such as the high heat (i.e., energy) requirement to release H₂S from the solvent, loss of alkanolamine due to its high volatility, transfer of water into the gas stream during the desorption step, and alkanolamine degradation to form corrosive compounds. These drawbacks make this treatment economically unattractive.^{12–14} Alternatively, H₂S physical absorbents present an important advantage of easier regeneration at lower temperatures compared to chemical absorbents. Some physical absorbents such as methanol, morpholine, and tetraglyme (TGM) are used in commercial products such as Selexol, Rectisol, and Morphysorb.¹⁵ However, the relatively high volatility of these compounds necessitates the search for new H₂S absorbents that can overcome the associated drawbacks.

Received: September 30, 2020

Revised: January 11, 2021

Published: January 28, 2021



For this reason, ionic liquids (ILs) have been proposed to replace these traditional solvents due to their excellent properties for gas separation applications¹⁶ including a high and tunable solvent capacity, low corrosivity, nonvolatility, low flammability, and relatively high thermal and chemical stability.^{16,17} Moreover, the possibility of tuning the cation and/or the anion for specific applications has led to ILs being described as “designer solvents.”¹⁸ The use of ILs to physically absorb H₂S has gained the interest of the scientific community in recent years, concluding that strong hydrogen bonding interactions between the IL anion and H₂S dominate over cation effects.^{19–28} A wide variety of studies has used COSMO-RS to select ILs with high solubility of H₂S, minimizing expensive and time-consuming experimental tests.^{29–35} However, one of the common drawbacks of ILs with high H₂S solubility is their high viscosity, which leads to mass transfer limitations during absorption operations.^{33,36} Less studied but thermodynamically much more attractive are ILs that chemically absorb H₂S. It was reported that ILs containing carboxylate groups are a class with excellent affinity toward H₂S because of their Lewis base features.^{37–39} However, their higher viscosities make them difficult to be applied at a larger scale.

In recent years, we have followed a multiscale research strategy using the COSMO-based/Aspen methodology, linking both molecular and process simulations to design novel gas absorption processes based on ILs.^{36,40–48} We have successfully demonstrated that mixing two ILs with positive deviations from ideality leads to absorbents with enhanced thermodynamics for CO₂ physical absorption.⁴⁹ In addition, recently, we demonstrated that it is possible to choose IL mixtures with low-viscosity organic solvents (such as TGM) to reduce the energy and solvent costs involved in CO₂ chemical absorption.⁵⁰ Based on these previous findings, the objective of this work is to use COSMO-RS and COSMO-based/Aspen computational tools to assess the performance of IL-based blends for H₂S capture. Our starting point was the formulation of new IL–IL mixtures with enhanced H₂S absorbent properties based on previous findings of IL-based blends with improved CO₂ absorption thermodynamics⁴⁹ and kinetics.⁵¹ An initial thermodynamic COSMO-RS study was carried out to find the synergic effects on nonideal performance of IL-based blends to improve the target H₂S absorbent properties (Henry’s constant) with respect to the neat ILs. The thermodynamic behavior for H₂S absorption of the selected IL-based blends was compared to their diffusion coefficients, a key kinetic parameter. Subsequently, the IL-based blends’ performance was assessed at the process scale, evaluating the H₂S physical absorption in a commercial packed column using the COSMO-based/Aspen methodology. The process simulation analysis with IL-based blends also involved an IL with chemical absorption by H₂S, 1-butyl-3-methylimidazolium acetate ([Bmim][OAc]), and an organic cosolvent (TGM) with low viscosity, with the aim of improving both absorption thermodynamics and kinetics in the selection of the most viable IL-based blend as a H₂S absorbent. The main aim of this computational analysis was to find new IL-based formulations with enhanced H₂S absorbent properties. In the future, equipment design, operating conditions, and process configurations could be improved to support the economic and technical viability of the proposed separation process based on IL blends.^{52,53}

■ COMPUTATIONAL DETAILS

COSMO-RS Calculations. The molecular structure of the selected ILs was defined by the ion-paired model using COSMO-RS calculations.⁵⁴ First, IL geometric structures were optimized to the minimum energy level at a computational level of BP-TZVP, including solvent effects through the COSMO continuum solvation model.⁵⁵ Vibrational frequencies were calculated to check the presence of an energy minimum during geometric optimization. We then generated a “.cosmo” file including the charge distributions of each compound to use in COSMOtherm software to calculate the thermophysical properties of the fluid.⁵⁶ TURBOMOLE (V 4.1.1)⁵⁷ and COSMOtherm (version C30_1701) programs were used for these calculations. COSMO-RS calculations were carried out using BP_TZVP_C30_1701 as implicit parameterization.

H₂S Henry’s law constants in neat ILs or equimolar IL-based blends were obtained at 298 K. First, the Henry’s law constant (K_{Henry}) was obtained using eq 1

$$K_{\text{Henry}} = \gamma_i^{\infty} \cdot p_0^{\text{vap}} \quad (1)$$

where K_{Henry} is the Henry’s law constant; γ_i^{∞} is the activity coefficient of H₂S in the IL at infinite dilution, and p_0^{vap} is the vapor pressure of the pure gas, obtained using the Antoine equation using experimental data.⁵⁸

Aspen Plus Process Simulations. The proposed H₂S capture unit was scaled up as a packed absorption column using the Aspen Plus commercial process simulator in order to assess H₂S separation from natural gas streams (Figure 1)

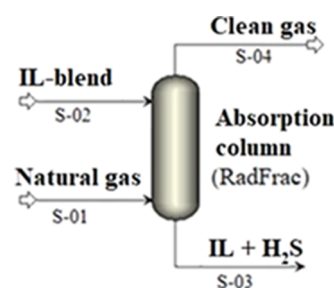


Figure 1. Simulated absorption column flow diagram.

using the neat ILs and diverse IL-based blends (25, 50, and 75% in weight) at pressures from 1 to 20 bar and isothermal operating conditions of 298 K (Table 1). ILs were included as pseudocomponents in the simulator along with all parameters needed to describe their H₂S physical and chemical absorption potential by applying a successful multiscale COSMO-based and Aspen Plus procedure, reinforced using experimental results^{37–39} as previously reported elsewhere.^{41,50,51} In the case of H₂S chemical absorption, H₂S–[Bmim][OAc] experimental isotherms³⁷ were successfully fitted to a thermodynamic model (see Figure S1 of the Supporting Information) in which the physical absorption is defined by Henry’s law constants and the chemical equilibrium reaction considers a 2:1 mechanism, where two IL ion pairs react with one H₂S molecule to form a complex of AB₂, as described elsewhere.^{50,51} Both quantum chemical structure optimizations and also COSMO-RS calculations of [Bmim][OAc] and products of its reaction with H₂S were performed to entirely specify the COSMOSAC property method, which is the property method utilized in our Aspen Plus calculations (code 1, COSMOSAC method by

Table 1. Column Properties, Operating Conditions, and Gas Stream Compositions Implemented in Aspen Plus

column properties			
height (m)		20	
packing type		Raschig rings	
number of stages		10	
operating conditions			
solvent mass flow (t/h)		250	
IL–IL mixture (% mass)		0, 2S, 50, 7S, and 100	
temperature (K)		298	
pressure (bar)		1, 5, 10, 15, and 20	
component	MW, kg/kmol	y _i	flow, kmol/h
CH ₄	16	0.940	1222.9
CO ₂	44	0.025	32.5
N ₂	14	0.015	19.5
H ₂ S	34	0.020	26.1

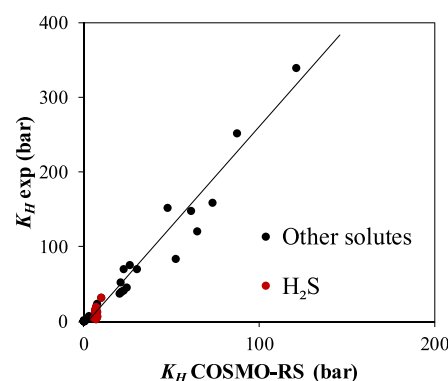
Sandler et al.⁵⁹). The thermodynamic, chemical reaction, and kinetic parameters used to define the systems involving [Bmim][OAc] in Aspen Plus are summarized in Table S1 of the Supporting Information. The information generated by a priori DFT and COSMO-RS computational methods (molecular weight, density, boiling point, molecular volume, and sigma profiles) to specify the COSMOSAC property model is also included. Regarding [Bmim][OAc], the same pure compound information is included, along with that for the reactants and the products of the reaction with H₂S. The required information to describe [Bmim][OAc] chemical absorption of H₂S and CO₂ (equilibrium constants and enthalpies of reaction) is also listed in Table S1 of the Supporting Information. The other ILs involved in the simulations, which just physically absorb H₂S, were added using the ILUAM database⁴¹ and their H₂S solubility was described by the COSMOSAC model.

The absorption unit was designed as a packed column, and the performance was evaluated using the RADFRAC rigorous model included in Aspen Plus v10 by default. Calculations were performed in the rate-based mode to consider the H₂S mass transfer kinetic process. The Aspen Plus reactive-distillation equilibrium reaction type was used to introduce [Bmim][OAc] chemical reactions.⁵⁰ The inlet natural gas and fresh solvent (neat IL or IL-based blends) streams were fed using given mass flow rates of 22.5 and 250 ton/h, respectively.⁴⁴ The inlet temperature and the total pressure of these gas and IL streams were 298 K and from 1 to 20 bar, respectively. The rate-based column height was 20 m, and the diameter was calculated using a fractional approach up to a maximum capacity of 65%. Raschig rings were selected as the packing for the absorption column.³³ The influences of operating pressure (varied from 1 to 20 bar) and IL-based blends on the H₂S uptake were analyzed. The H₂S recovery achieved was calculated to evaluate the absorption efficiency. Table 1 lists the details of the typical parameters and operating conditions for the simulations carried out.

RESULTS AND DISCUSSION

Absorbent Property Analysis by COSMO-RS. The first step in the simulation study was the validation of the ability of COSMO-RS to predict H₂S solubility in the ILs. This analysis was recently reported,^{33,40} involving the Henry's law constant values of H₂S in pure ILs (K_{Henry}) for different systems at nearly ambient temperatures, covering a range of gas

solubilities.³³ Figure 2 shows the correlation of experimental data and predictions by COSMO-RS for a wide variety of

**Figure 2.** Henry's law constant prediction validation model of different solutes obtained using COSMO-RS calculations at 298 K.

solutes (carbon dioxide, ammonia, alkanes, etc.) with ILs, including those with H₂S, marked with red symbols in Figure 2 (data in Table S2 of the Supporting Information).^{19–27} These data provided a reasonable qualitative prediction (R^2 of 0.97). The corrected COSMO-RS computational approach provides a mean percentage error of 7.62% for the 16 $K_{\text{Henry}}^{\text{H}_2\text{S}}$ values of H₂S–IL systems using the [CA] model to describe the IL.

$$K_{\text{H,Exp}}^{\text{H}_2\text{S}} = 2.66 \cdot K_{\text{H,COSMO-RS}}^{\text{H}_2\text{S}} - 5.47 \quad (2)$$

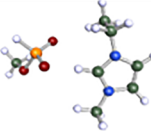
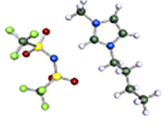
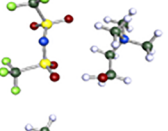
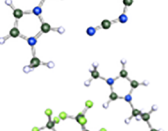
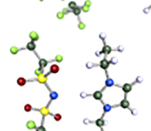
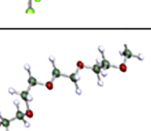
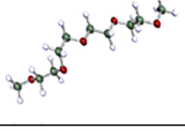
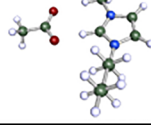
Equation 2 shows the linear correlation obtained from Figure 2. The calculated K_{Henry} values by COSMO-RS were corrected using eq 2 in this work in order to increase the quantitative accuracy of the predictions.

Different IL-based blends with [Emim][(MeO)PO₂H] as the common component (Table 2) were initially nominated to examine the effects of a characteristic sample of mixture on H₂S solubilities. [Emim][(MeO)PO₂H] was selected as the common IL₁ as it was previously reported to be one of the most thermodynamically promising ILs for H₂S absorption,³³ presenting one of the lowest K_{Henry} value (Table 2). However, a disadvantage for the industrial application of [Emim]–[(MeO)PO₂H] is its high viscosity (149.1 cP at 298 K),⁶⁰ which will complicate mass transport during the capture of H₂S, implying higher IL consumption. Therefore, our proposal to solve this limitation is to blend it with other ILs (Table 2) to significantly improve the transport properties of the absorbent, while maintaining, or even enhancing, its absorption capacity through synergistic mixing effects.

Once the preliminary selection was completed, the thermodynamics of H₂S absorption in these IL-based blends was analyzed using the Henry's constant values (K_{Henry}). Figure 3 shows the K_{Henry} values of [Emim][(MeO)PO₂H]–absorbent₂ mixtures at different molar fractions and 298 K. It was observed that the lowest value of K_{Henry} corresponds to the neat [Emim][(MeO)PO₂H] (under 10 bar), with this value increasing when the absorbent₂ content increases, which implies lower H₂S solubility in the mixed absorbents.

Once we had analyzed the global thermodynamic behavior of the IL-based blends for H₂S absorption, the potential synergic effects on IL-based blends were analyzed in more detail. With this aim, the Henry's law constant deviations from ideality for IL-based blends ($\Delta H_{K_{\text{Henry}}}^{\text{H}_2\text{S}}$) were estimated as a parameter of reference of nonideal mixing effects.⁴⁹ $\Delta H_{K_{\text{Henry}}}^{\text{H}_2\text{S}}$ is

Table 2. Structures and Physical, Chemical, and Thermodynamic Values of the Selected ILs and TGM Measured at 298 K Using ILThermo Website

Ionic liquid	Structure	$K_{\text{H, COSMO-RS}}$ (bar)	$K_{\text{H, Linear}}$ (bar)	$\Delta K_{\text{H}}^{\text{H}_2\text{S}}$ (bar)	$\gamma_{\text{IL-IL}}$	$\mu_{\text{IL-IL}}$	$\mu_{\text{improvement}}$ (%)
[Emim][(MeO)PO ₂ H]		8.8	8.8	--	0.89	149.1	--
[Bmim][NTf ₂]		10.0	10.0	0.02	1.06	87.5	41.3
[Choline][NTf ₂]		11.2	10.3	0.89	0.28	118.4	20.6
[Emim][DCN]		11.9	12.2	-0.31	2.04	50.1	66.4
[Hmim][FEP]		9.4	9.6	-0.25	>2.5	111.5	25.2
[Emim][BETi]		8.9	9.2	-0.26	2.14	120.9	18.9
TGM		9.0	10.1	-1.06	>2.5	21.2	85.8
[Bmim][OAc]		9.2	9.2	0.03	1.15	258.3	-73.2

calculated as the change of the predicted and corrected data from COSMO-RS ($K_{\text{Henry, IL-abs, COSMO-RS}}^{\text{H}_2\text{S}}$) and the data estimated from the linear (mixture) performance obtained from K_{Henry} of the neat absorbents ($K_{\text{Henry, IL-abs, Linear}}^{\text{H}_2\text{S}}$), which is given as eq 3.

$$\left(\Delta H = \frac{H_2\text{S}}{K_{\text{Henry}}} \right) = K_{\text{Henry, IL-abs, COSMO-RS}}^{\text{H}_2\text{S}} - K_{\text{Henry, IL-abs, Linear}}^{\text{H}_2\text{S}} \quad (3)$$

Figure 4 shows the Henry's law constant mixing deviations of H₂S in equimolar IL-based blends ($\Delta K_{\text{Henry}}^{\text{H}_2\text{S}}$) for more than 400 equimolar [Emim][(MeO)PO₂H]–IL₂ mixtures and [Emim][(MeO)PO₂H]–TGM mixtures plotted against the activity coefficient of [Emim][(MeO)PO₂H] (Figure 4A) in the IL-based blends. In good agreement with the conclusions of the Shulgin model,⁶¹ a relationship between $\Delta K_{\text{Henry}}^{\text{H}_2\text{S}}$ in IL-based blends and the reference activity coefficient of the absorbents in the equimolar IL-based blends was found

($\gamma_{[\text{Emim}][(\text{MeO})\text{PO}_2\text{H}]}$). Thus, the solvent mixing effect on H₂S solubility could be openly classified in a thermodynamic context. IL-based blends showing a nearly ideal mixture behavior ($\gamma_{\text{IL}} \sim 1$) present H₂S solubility almost equal to the average of the pure absorbents, in other words, an additive performance in their constant of Henry values ($\Delta K_{\text{Henry}}^{\text{H}_2\text{S}} \sim 0$). In contrast, those IL-based blends showing positive deviations from ideality ($\gamma_{\text{IL}} > 1$, the green zone of Figure 4A) due to nonfavorable blending properties, because of unfavorable intermolecular interactions between the solvents or diminishing entropy, could present significantly improved H₂S solubilities ($\Delta K_{\text{Henry}}^{\text{H}_2\text{S}} < 0$) compared to the behavior of the pure absorbents. On the other hand, those IL-based blend components with good performance (giving $\gamma_{\text{IL}} < 1$, the red zone of Figure 4A) might not be good candidates as H₂S absorbents as the H₂S–solvent interaction could be hindered by IL–IL interactions, giving unfavorable $\Delta K_{\text{Henry}}^{\text{H}_2\text{S}}$ values, higher than zero. Regarding the preliminary selected IL-based blends (Table 2), Figure 4B shows the $\Delta K_{\text{Henry}}^{\text{H}_2\text{S}}$ values in IL-

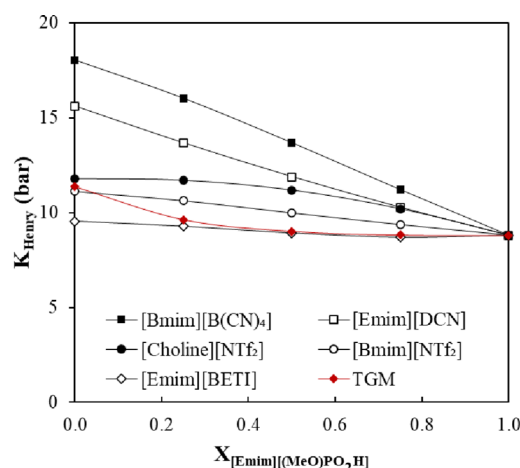


Figure 3. Henry's constant values (K_{Henry} , bar) of H_2S in blends of $[\text{Emim}][(\text{MeO})\text{PO}_2\text{H}]$ with other ILs and TGM (see details in the inset) calculated using COSMO-RS at 298 K.

based blends at different IL compositions, with the aim of finding synergic mixture effects. $[\text{Emim}][(\text{MeO})\text{PO}_2\text{H}]$ also showed synergic effects with $[\text{Hmim}][\text{FEP}]$, $[\text{Emim}][\text{BETI}]$, $[\text{Emim}][\text{DCN}]$ and, to a greater extent, TGM, so the list of the previously selected ILs is reduced (Table 2) to $[\text{Emim}][(\text{MeO})\text{PO}_2\text{H}]$ – $[\text{Emim}][\text{DCN}]$ and $[\text{Emim}][(\text{MeO})\text{PO}_2\text{H}]$ –TGM.

After we analyzed the thermodynamic behavior of the IL-based blends for H_2S absorption, their viscosity was studied as a kinetic parameter of reference for $[\text{Emim}][(\text{MeO})\text{PO}_2\text{H}]$ –absorbent₂ mixtures. The viscosity of IL–absorbent binary mixtures was obtained from absolute experimental viscosities using the mixing law of Grunberg and Nissan,⁶² as follows

$$\text{Log}_{10}(\mu) = x_1 \cdot \text{Log}_{10}(\mu_1) + x_2 \cdot \text{Log}_{10}(\mu_2) \quad (4)$$

Table 3 shows the predictions of corrected K_{Henry} values using COSMO-RS ($K_{\text{H, COSMO-RS}}$), equimolar K_{Henry} estimated by linear regression between the two absorbents ($K_{\text{H, Linear}}$), the Henry's law constant deviations ($\Delta K_{\text{H}}^{\text{H}_2\text{S}}$), equimolar activity coefficient of the IL-based blends ($\gamma_{\text{IL-abs}}$), the estimated equimolar values of viscosity of the blend ($\mu_{\text{IL-abs}}$, eq 4), and viscosity improvements with respect to $[\text{Emim}][(\text{MeO})\text{PO}_2\text{H}]$ ($\mu_{\text{improvement}}$) for all of the selected systems. It

is observed that the IL-based blends $[\text{Emim}][(\text{MeO})\text{PO}_2\text{H}]$ –TGM and $[\text{Emim}][(\text{MeO})\text{PO}_2\text{H}]$ – $[\text{Emim}][\text{DCN}]$ present both favorable thermodynamics and kinetics for H_2S absorption. The mass solubility (mg/g), obtained from K_{Henry} , and diffusivity (m^2/s), obtained using the Wilke–Chang equation,³⁶ were compared as shown in Figure 5, with opposite trends observed for H_2S absorption thermodynamics and kinetics of the mixture compositions. Neat $[\text{Emim}][(\text{MeO})\text{PO}_2\text{H}]$ presents the highest mass solubility but the lowest diffusivity. Therefore, increasing the amount of the other solvent enhances the absorbent transport properties but decreases the H_2S gas solubility. Therefore, it is required to analyze these IL-based blends using process simulations in order to evaluate the role of thermodynamics and kinetics in process performance.

Separation Process Performance Evaluated using Aspen Plus. After we analyzed the key thermodynamic/kinetic properties of H_2S absorption in IL-based blends by molecular simulations, we employed a COSMO-based/Aspen methodology in order to assess the performance of the selected IL-based mixtures for absorption of H_2S from a characteristic acid natural gas stream (Table 1) using commercial packed columns. Previous process simulations revealed a determinant effect of the mass transport properties of ILs on the efficiency of H_2S recovery³³ and CO_2 absorption processes.^{36,44,63} In the case of H_2S capture, all of the selected ILs (Table 2) present reasonably high solubilities (K_{Henry} values between 8.8 and 18 bar), so the strategy in the process simulation was to combine the selected ILs with solvents of lower viscosity. Thus, the equimolar mixtures of $[\text{Emim}][(\text{MeO})\text{PO}_2\text{H}]$ with $[\text{Emim}][\text{DCN}]$ and TGM gave a decrease in the viscosity of 66.4 and 85.8%, respectively, compared to neat $[\text{Emim}][(\text{MeO})\text{PO}_2\text{H}]$ (Table 3).

For absorption using a packed column, the rigorous model of a RADFRAC column using the rate-based mode was used for a more realistic setup, taking into account both the thermodynamic and kinetic effects on the H_2S separation efficiency by IL mixtures. Figure 6A shows the comparison of the percentage of H_2S recovery using $[\text{Emim}][(\text{MeO})\text{PO}_2\text{H}]$ – $[\text{Emim}][\text{DCN}]$ mixtures with different compositions at different operating pressures. The highest H_2S recovery was achieved using pure $[\text{Emim}][\text{DCN}]$, which presents the lowest viscosity. An increase in the operating pressure from 1 to 20 bar results in significantly higher H_2S capture (Figure 6A) due

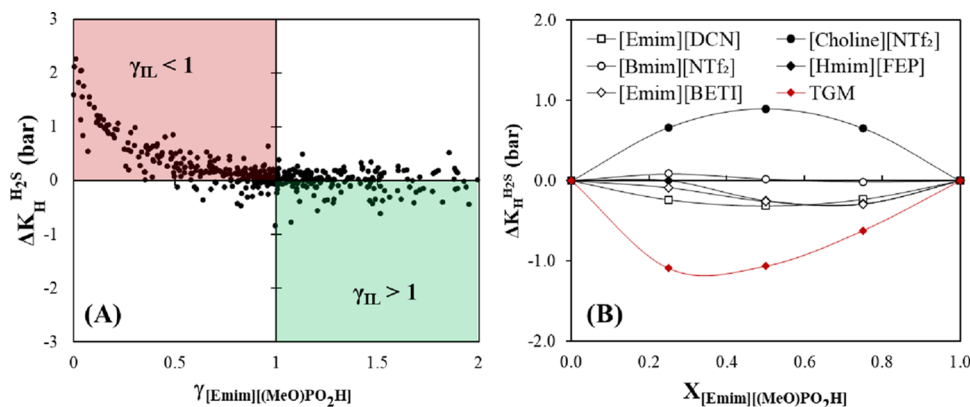


Figure 4. Henry's law constant mixing deviations of H_2S ($\Delta K_{\text{H}}^{\text{H}_2\text{S}}$, bar) versus activity coefficients in equimolar $[\text{Emim}][(\text{MeO})\text{PO}_2\text{H}]$ mixtures (γ_{IL}) (A) and Henry's law constant deviation of H_2S ($\Delta K_{\text{H}}^{\text{H}_2\text{S}}$, bar) in $[\text{Emim}][(\text{MeO})\text{PO}_2\text{H}]$ mixtures with other absorbents (see details in the inset) (B), obtained using COSMO-RS at 298 K.

Table 3. Henry Constant Values of H₂S (Obtained using COSMO-RS and by Linear Behavior of each IL Making the Mixture), the Activity Coefficient, and Viscosity (and its Improvement with Respect to [Emim][(MeO)PO₂H]) of Equimolar IL-Based Blends at 298 K

ionic liquid	$K_{\text{H, COSMO-RS}}$ (bar)	$K_{\text{H, Linear}}$ (bar)	$\Delta K_{\text{H}}^{\text{H}_2\text{S}}$ (bar)	$\gamma_{\text{IL-abs}}$	$\mu_{\text{IL-abs}}$ (cP)	$\mu_{\text{improvement}}$ (%)
[Emim][(MeO)PO ₂ H]	8.8	8.8		0.89	149.1	
[Bmim][NTf ₂]	10.0	10.0	0.02	1.06	87.5	41.3
[Choline][NTf ₂]	11.2	10.3	0.89	0.28	118.4	20.6
[Emim][DCN]	11.9	12.2	−0.31	2.04	50.1	66.4
[Hmim][FEP]	9.4	9.6	−0.25	>2.5	111.5	25.2
[Emim][BETi]	8.9	9.2	−0.26	2.14	120.9	18.9
TGM	9.0	10.1	−1.06	>2.5	21.2	85.8
[Bmim][OAc]					258.3	−73.2

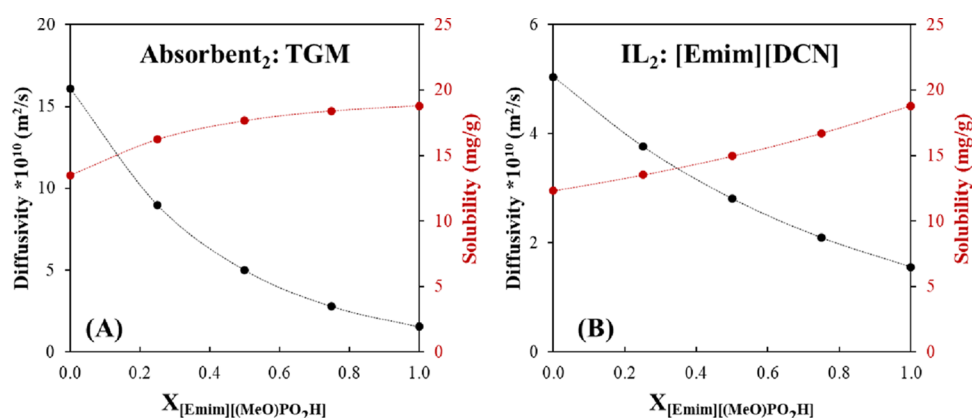


Figure 5. H₂S solubility and diffusivity obtained from the Wilke–Chang equation for two IL-based blends at 298 K and 1 bar for (A) [Emim][(MeO)PO₂H]–TGM and (B) [Emim][(MeO)PO₂H]–[Emim][DCN].

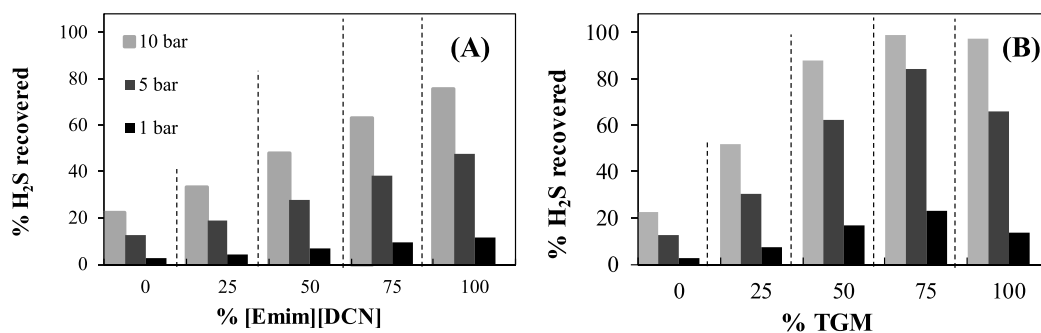


Figure 6. Percentage of H₂S recovered using (A) [Emim][(MeO)PO₂H]–[Emim][DCN] and (B) [Emim][(MeO)PO₂H]–TGM for different mixture ratios at 250 ton/h of the absorbent mixture in absorption packed columns, obtained at the operating conditions listed in Table 1.

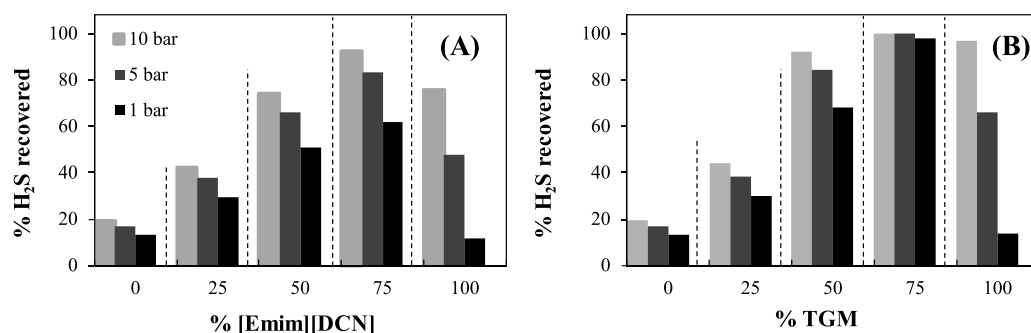


Figure 7. Percentage of H₂S recovered using (A) [Bmim][OAc]–[Emim][DCN] and (B) [Bmim][OAc]–TGM for different mixture ratios at 250 ton/h of the absorbent blend in an absorption packed column, obtained at the operating conditions listed in Table 1.

to the increased gas solubility but the kinetic control of H₂S absorption remains constant, which means, the determinant influence of IL viscosity. In summary, we did not succeed in formulating IL–IL blends with enhanced thermodynamic/kinetic properties for H₂S physical absorption, obtaining the best behavior with the pure ILs with the lowest viscosity. In the case of the [Emim][(MeO)PO₂H]–TGM blend (Figure 6B), the maximum H₂S recovery was found at 75% (w/w) of TGM, evident of a synergistic effect between these two absorbents. Moreover, at 10 bar, we predicted 99% H₂S recovery at 25/75 for [Emim][(MeO)PO₂H]–TGM.

In order to obtain a more favorable IL-based blend to capture H₂S, we evaluated [Bmim][OAc] as a H₂S chemical absorbent in a packed column. [Bmim][OAc] is characterized by a remarkably high H₂S absorption capacity (compared to ILs with physical absorption of H₂S) although poor mass transport properties were found due to its high viscosity (Tables 2 and 3).⁵⁰ Thus, [Bmim][OAc] was mixed with [Emim][DCN], the IL with the lowest viscosity, in the current study. Figure 7A shows the H₂S recovery at different IL–IL compositions and different pressures. Remarkably, in this case, we found an IL–IL blend with an enhanced H₂S absorbent behavior with respect to the neat ILs, that is, a new IL-based formulation with a favorable compromise between thermodynamics and kinetics for H₂S absorption. An IL–IL blend of 75% of [Emim][DCN] at 10 bar of pressure offers the maximum H₂S recovery (> 98%). [Bmim][OAc] was also mixed with TGM, a low-viscosity solvent used industrially as a physical absorbent of acid gases (CO₂, H₂S, NO_x, or SO₂). Recently, TGM was successfully used as a cosolvent with carboxylate-based ILs to minimize the mass transfer limitations in CO₂ chemical absorption.⁵¹ Figure 7B shows the simulated performance of [Bmim][OAc]–TGM blends for H₂S capture in a commercial packed column. Considering the different ratios of the blend, there is a clear synergistic effect, with higher H₂S recovery at any mixture composition. The best results were achieved at a TGM composition of 75% in weight, yielding 98% of H₂S recovery at 1 bar, a remarkably better performance than not only the [Bmim][OAc]–[Emim][DCN] blends but also the best [Emim][(MeO)PO₂H]–TGM blend (Figure 6B). This result is explained by the synergistic effects of the mixture having high [Bmim][OAc] absorption capacity and low viscosity of TGM. In terms of the economics of the process, this result would drastically reduce the consumption of ILs using the cosolvent TGM. Moreover, IL-based blends are presented as alternatives to aqueous amine solutions, widely used in industries, preventing some drawbacks such as volatile losses, intensive energy consumption to regenerate the absorbent, and the formation of corrosive byproducts.

CONCLUSIONS

The integration of COSMO-RS molecular simulations and thermodynamic analysis offers new insights into the efficacy of blending ILs for H₂S solubility. This paper confirmed the synergistic H₂S solubility effect found by blending two solvents which combine positive deviations from ideality. It should be highlighted that these IL-based blends frequently give favorable gas solubilities with unfavorable mass transfer kinetics. These consequences provided opportunities to propose new absorbents with well-balanced kinetic and thermodynamic properties for H₂S absorption.

The absorption operation was simulated for IL-based blends to assess their performance in both physical and chemical H₂S capture processes using a COSMO-based/Aspen Plus methodology using typical natural gas streams of industrial plants, with a column height of 20 m, a given mass flow of 22.5 ton/h of natural gas, and 250 ton/h of absorbent at 298 K. The solvent viscosity was found as the key property that defines the IL behavior for H₂S absorption. The results indicate that blending of [Bmim][OAc]—a H₂S chemical absorbent—with a low viscosity solvent, for instance, TGM, provides excellent candidates for H₂S absorption, exhibiting better performance in absorption columns than the pure compounds, due to their compromise between favorable transport properties and high absorption capacities.

ASSOCIATED CONTENT

Supporting Information

The Supporting Information is available free of charge at <https://pubs.acs.org/doi/10.1021/acssuschemeng.0c07229>.

Detailed information on the validation of the H₂S–[Bmim][OAc] molar solubility at 1 bar and different temperatures, thermodynamic parameter to specify [Bmim][OAc] and its reaction products in Aspen Plus, and physicochemical and thermodynamic properties of the ILs previously studied (PDF)

AUTHOR INFORMATION

Corresponding Author

Jesús Lemus – Chemical Engineering Department, Universidad Autónoma de Madrid, Madrid 28049, Spain; orcid.org/0000-0001-5386-2868; Email: jesus.lemus@uam.es

Authors

Rubén Santiago – Chemical Engineering Department, Universidad Autónoma de Madrid, Madrid 28049, Spain; orcid.org/0000-0002-6877-9001

Daniel Hospital-Benito – Chemical Engineering Department, Universidad Autónoma de Madrid, Madrid 28049, Spain

Tom Welton – Imperial College London, London SW7 2AZ, U.K.

Jason P. Hallett – Imperial College London, London SW7 2AZ, U.K.; orcid.org/0000-0003-3431-2371

José Palomar – Chemical Engineering Department, Universidad Autónoma de Madrid, Madrid 28049, Spain; orcid.org/0000-0003-4304-0515

Complete contact information is available at: <https://pubs.acs.org/doi/10.1021/acssuschemeng.0c07229>

Notes

The authors declare no competing financial interest.

ACKNOWLEDGMENTS

Financial support from Ministerio de Economía y Competitividad of Spain (project CTQ2017-89441-R) and Comunidad de Madrid (project P2018/EMT4348) is acknowledged. Computational facilities provided by Centro de Computación Científica de la Universidad Autónoma de Madrid (UAM) is acknowledged.

REFERENCES

- (1) Chiappe, C.; Pomelli, C. S. Hydrogen Sulfide and Ionic Liquids: Absorption, Separation, and Oxidation. *Top. Curr. Chem. (Z)* **2017**, *375*, 52.
- (2) Shah, M. S.; Tsapatsis, M.; Siepmann, J. I. Hydrogen Sulfide Capture: From Absorption in Polar Liquids to Oxide, Zeolite, and Metal-Organic Framework Adsorbents and Membranes. *Chem. Rev.* **2017**, *117*, 9755–9803.
- (3) Kidnay, A. J.; Parrish, W. R., *Fundamentals of Natural Gas Processing*. CRC Press: 2006.
- (4) Ozekmekci, M.; Salkic, G.; Fellah, M. F. Use of zeolites for the removal of H₂S: A mini-review. *Fuel Process. Technol.* **2015**, *139*, 49–60.
- (5) Peters, L.; Hussain, A.; Follmann, M.; Melin, T.; Hägg, M. B. CO₂ removal from natural gas by employing amine absorption and membrane technology—A technical and economical analysis. *Chem. Eng. J.* **2011**, *172*, 952–960.
- (6) Bandosz, T. J. On the adsorption/oxidation of hydrogen sulfide on activated carbons at ambient temperatures. *J. Colloid Interface Sci.* **2002**, *246*, 1–20.
- (7) Florent, M.; Policicchio, A.; Niewiadomski, S.; Bandosz, T. J. Exploring the options for the improvement of H₂S adsorption on sludge derived adsorbents: Building the composite with porous carbons. *J. Cleaner Prod.* **2020**, *249*, No. 119412.
- (8) Sigot, L.; Ducom, G.; Germain, P. Adsorption of hydrogen sulfide (H₂S) on zeolite (Z): Retention mechanism. *Chem. Eng. J.* **2016**, *287*, 47–53.
- (9) Zhou, L.; Yu, M.; Zhong, L.; Zhou, Y., *Feasibility study on pressure swing sorption for removing H₂S from natural gas*. 2004; *59*, 2401–2406.
- (10) Shoukat, U.; Pinto, D.; Knuutila, H. Study of Various Aqueous and Non-Aqueous Amine Blends for Hydrogen Sulfide Removal from Natural Gas. *Processes* **2019**, *7*, No. 160.
- (11) Abd, A. A.; Naji, S. Z. Comparison study of activators performance for MDEA solution of acid gases capturing from natural gas: Simulation-based on a real plant. *Environ. Technol. Innov.* **2020**, *17*, No. 100562.
- (12) Galán Sánchez, L. M.; Meindersma, G. W.; de Haan, A. B. Solvent Properties of Functionalized Ionic Liquids for CO₂ Absorption. *Chem. Eng. Res. Design* **2007**, *85*, 31–39.
- (13) Bara, J. E., Potential for Hydrogen Sulfide Removal Using Ionic Liquid Solvents. In *Green Solvents II: Properties and Applications of Ionic Liquids*, Mohammad, A.; Inamuddin, D., Eds. Springer Netherlands: Dordrecht, 2012; 155–167.
- (14) Haider, J.; Saeed, S.; Qyyum, M. A.; Kazmi, B.; Ahmad, R.; Muhammad, A.; Lee, M. Simultaneous capture of acid gases from natural gas adopting ionic liquids: Challenges, recent developments, and prospects. *Renew. Sustainable Energy Rev.* **2020**, *123*, No. 109771.
- (15) Burr, B.; Lyddon, L., *A Comparison of Physical Solvents for Acid Gas Removal*. 2008; Vol. 1.
- (16) Wilkes, J. S.; Wasserscheid, P.; Welton, T., *Ionic Liquids in Synthesis*. Wiley-VCH Verlag GmbH & Co. KGaA: 2008; 1–6.
- (17) Welton, T. Ionic liquids: a brief history. *Biophys. Rev.* **2018**, *10*, 691–706.
- (18) Shang, D.; Liu, X.; Bai, L.; Zeng, S.; Xu, Q.; Gao, H.; Zhang, X. Ionic liquids in gas separation processing. *Curr. Opin. Green Sustain. Chem.* **2017**, *5*, 74–81.
- (19) Pomelli, C. S.; Chiappe, C.; Vidis, A.; Laurenczy, G.; Dyson, P. J. Influence of the Interaction between Hydrogen Sulfide and Ionic Liquids on Solubility: Experimental and Theoretical Investigation. *J. Phys. Chem. B* **2007**, *111*, 13014–13019.
- (20) Aparicio, S.; Atilhan, M. Computational Study of Hexamethylguanidinium Lactate Ionic Liquid: A Candidate for Natural Gas Sweetening. *Energy Fuels* **2010**, *24*, 4989–5001.
- (21) Jou, F.-Y.; Mather, A. E. Solubility of Hydrogen Sulfide in [bmim][PF₆]. *Int. J. Thermophys.* **2007**, *28*, 490.
- (22) Jalili, A. H.; Rahmati-Rostami, M.; Ghotbi, C.; Hosseini-Jenab, M.; Ahmadi, A. N. Solubility of H₂S in Ionic Liquids [bmim][PF₆], [bmim][BF₄], and [bmim][Tf₂N]. *J. Chem. Eng. Data* **2009**, *54*, 1844–1849.
- (23) Jalili, A. H.; Mehdizadeh, A.; Shokouhi, M.; Ahmadi, A. N.; Hosseini-Jenab, M.; Fateminassab, F. Solubility and diffusion of CO₂ and H₂S in the ionic liquid 1-ethyl-3-methylimidazolium ethylsulfate. *J. Chem. Thermodyn.* **2010**, *42*, 1298–1303.
- (24) Shiflett, M. B.; Niehaus, A. M. S.; Yokozeeki, A. Separation of CO₂ and H₂S Using Room-Temperature Ionic Liquid [bmim][MeSO₄]. *J. Chem. Eng. Data* **2010**, *55*, 4785–4793.
- (25) Zhao, Y.; Gao, H.; Zhang, X.; Huang, Y.; Bao, D.; Zhang, S. Hydrogen Sulfide Solubility in Ionic Liquids (ILs): An Extensive Database and a New ELM Model Mainly Established by Imidazolium-Based ILs. *J. Chem. Eng. Data* **2016**, *61*, 3970–3978.
- (26) Jalili, A. H.; Mehrabi, M.; Zoghi, A. T.; Shokouhi, M.; Taheri, S. A. Solubility of carbon dioxide and hydrogen sulfide in the ionic liquid 1-butyl-3-methylimidazolium trifluoromethanesulfonate. *Fluid Phase Equilibria* **2017**, *453*, 1–12.
- (27) Jalili, A. H.; Shokouhi, M.; Maurer, G.; Zoghi, A. T.; Sadeghzah Ahari, J.; Forsat, K. Measuring and modelling the absorption and volumetric properties of CO₂ and H₂S in the ionic liquid 1-ethyl-3-methylimidazolium tetrafluoroborate. *J. Chem. Thermodyn.* **2019**, *131*, 544–556.
- (28) Zhang, X.; Xiong, W.; Peng, L.; Wu, Y.; Hu, X. Highly selective absorption separation of H₂S and CO₂ from CH₄ by novel azole-based protic ionic liquids. *AIChE J.* **2020**, *66*, 1547–5905.
- (29) Zhao, Y.; Gao, J.; Huang, Y.; Afzal, R. M.; Zhang, X.; Zhang, S. Predicting H₂S solubility in ionic liquids by the quantitative structure-property relationship method using S sigma-profile molecular descriptors. *RSC Adv.* **2016**, *6*, 70405–70413.
- (30) Kamgar, A.; Esmailzadeh, F. Prediction of H₂S solubility in hmim Pf(6), hmim Bf(4) and hmim Tf₂N using UNIQUAC, NRTL and COSMO-RS. *J. Mol. Liq.* **2016**, *220*, 631–634.
- (31) Mortazavi-Manesh, S.; Satyro, M. A.; Marriott, R. A. Screening ionic liquids as candidates for separation of acid gases: Solubility of hydrogen sulfide, methane, and ethane. *AIChE J.* **2013**, *59*, 2993–3005.
- (32) Carvalho, P. J.; Coutinho, J. A. P. Non-ideality of Solutions of NH₃, SO₂, and H₂S in Ionic Liquids and the Prediction of Their Solubilities Using the Flory–Huggins Model. *Energy Fuels* **2010**, *24*, 6662–6666.
- (33) Santiago, R.; Lemus, J.; Outomuro, A. X.; Bedia, J.; Palomar, J. Assessment of ionic liquids as H₂S physical absorbents by thermodynamic and kinetic analysis based on process simulation. *Sep. Purific. Technol.* **2020**, *233*, No. 116050.
- (34) Zhao, Z.; Huang, Y.; Zhang, Z.; Fei, W.; Luo, M.; Zhao, Y. Experimental and simulation study of CO₂ and H₂S solubility in propylene carbonate, imidazolium-based ionic liquids and their mixtures. *J. Chem. Thermodyn.* **2020**, *142*, No. 106017.
- (35) Mesbah, M.; Soroush, E.; Momeni, M.; Shahsavari, S.; Mofidi, M.; Soltanali, S. Rigorous correlations for predicting the solubility of H₂S in methylimidazolium-based ionic liquids. *Can. J. Chem. Eng.* **2019**, *98*, 441–452.
- (36) Palomar, J.; Larriba, M.; Lemus, J.; Moreno, D.; Santiago, R.; Moya, C.; de Riva, J.; Pedrosa, G. Demonstrating the key role of kinetics over thermodynamics in the selection of ionic liquids for CO₂ physical absorption. *Sep. Purific. Technol.* **2019**, *213*, 578–586.
- (37) Huang, K.; Cai, D.-N.; Chen, Y.-L.; Wu, Y.-T.; Hu, X.-B.; Zhang, Z.-B. Thermodynamic validation of 1-alkyl-3-methylimidazolium carboxylates as task-specific ionic liquids for H₂S absorption. *AIChE J.* **2013**, *59*, 2227–2235.
- (38) Haghtalab, A.; Kheiri, A. High pressure measurement and CPA equation of state for solubility of carbon dioxide and hydrogen sulfide in 1-butyl-3-methylimidazolium acetate. *J. Chem. Thermodyn.* **2015**, *89*, 41–50.
- (39) Zhao, T.; Li, P.; Feng, X.; Hu, X.; Wu, Y. Study on absorption and spectral properties of H₂S in carboxylate protic ionic liquids with low viscosity. *J. Mol. Liq.* **2018**, *266*, 806–813.
- (40) Santiago, R.; Bedia, J.; Moreno, D.; Moya, C.; de Riva, J.; Larriba, M.; Palomar, J. Acetylene absorption by ionic liquids: A

multiscale analysis based on molecular and process simulation. *Sep. Purific. Technol.* **2018**, 204, 38–48.

(41) Ferro, V. R.; Moya, C.; Moreno, D.; Santiago, R.; de Riva, J.; Pedrosa, G.; Larriba, M.; Diaz, I.; Palomar, J. Enterprise Ionic Liquids Database (ILUAM) for Use in Aspen ONE Programs Suite with COSMO-Based Property Methods. *Ind. Eng. Chem. Res.* **2018**, 57, 980–989.

(42) Ferro, V. R.; Ruiz, E.; de Riva, J.; Palomar, J. Introducing process simulation in ionic liquids design/selection for separation processes based on operational and economic criteria through the example of their regeneration. *Sep. Purific. Technol.* **2012**, 97, 195–204.

(43) De Riva, J.; Roberto Ferro Fernandez, V.; Moya, C.; Stadtherr, M. A.; Brennecke, J. F.; Palomar, J. Aspen Plus supported analysis of the post-combustion CO₂ capture by chemical absorption using the [P2228][CNPyrr] and [P66614][CNPyrr] AHA Ionic Liquids. *Int. J. Greenhouse Gas Control* **2018**, 78, 94–102.

(44) de Riva, J.; Suarez-Reyes, J.; Moreno, D.; Diaz, I.; Ferro, V.; Palomar, J. Ionic liquids for post-combustion CO₂ capture by physical absorption: Thermodynamic, kinetic and process analysis. *Int. J. Greenhouse Gas Control* **2017**, 61, 61–70.

(45) Palomar, J.; Gonzalez-Miquel, M.; Polo, A.; Rodriguez, F. Understanding the Physical Absorption of CO₂ in Ionic Liquids Using the COSMO-RS Method. *Ind. Eng. Chem. Res.* **2011**, 50, 3452–3463.

(46) Palomar, J.; Gonzalez-Miquel, M.; Bedia, J.; Rodriguez, F.; Rodriguez, J. J. Task-specific ionic liquids for efficient ammonia absorption. *Sep. Purific. Technol.* **2011**, 82, 43–52.

(47) Fallanza, M.; González-Miquel, M.; Ruiz, E.; Ortiz, A.; Gorri, D.; Palomar, J.; Ortiz, I. Screening of RTILs for propane/propylene separation using COSMO-RS methodology. *Chem. Eng. J.* **2013**, 220, 284–293.

(48) Liu, X.; Ruiz, E.; Afzal, W.; Ferro, V.; Palomar, J.; Prausnitz, J. M. High Solubilities for Methane, Ethane, Ethylene, and Propane in Trimethyloctylphosphonium Bis(2,4,4-trimethylpentyl) Phosphinate ([P8111][TMPP]). *Ind. Eng. Chem. Res.* **2014**, 53, 363–368.

(49) Moya, C.; Gonzalez-Miquel, M.; Rodriguez, F.; Soto, A.; Rodriguez, H.; Palomar, J. Non-ideal behavior of ionic liquid mixtures to enhance CO₂ capture. *Fluid Phase Equilibria* **2017**, 450, 175–183.

(50) Hospital-Benito, D.; Lemus, J.; Moya, C.; Santiago, R.; Palomar, J. Process analysis overview of ionic liquids on CO₂ chemical capture. *Chem. Eng. J.* **2020**, 390, No. 124509.

(51) Hospital-Benito, D.; Lemus, J.; Santiago, R.; Palomar, J. Thermodynamic and kinetic evaluation of ionic liquids + tetraglyme mixtures on CO₂ capture. *J. CO₂ Util.* **2020**, 35, 185–193.

(52) de Riva, J.; Ferro, V. R.; Moreno, D.; Diaz, I.; Palomar, J. Aspen Plus supported conceptual design of the aromatic–aliphatic separation from low aromatic content naphtha using 4-methyl-N-butylpyridinium tetrafluoroborate ionic liquid. *Fuel Process. Technol.* **2016**, 146, 29–38.

(53) Moreno, D.; Ferro, V. R.; de Riva, J.; Santiago, R.; Moya, C.; Larriba, M.; Palomar, J. Absorption refrigeration cycles based on ionic liquids: Refrigerant/absorbent selection by thermodynamic and process analysis. *Appl. Energy* **2018**, 213, 179–194.

(54) Klamt, A. Conductor-like Screening Model for Real Solvents: A New Approach to the Quantitative Calculation of Solvation Phenomena. *J. Phys. Chem.* **1995**, 99, 2224–2235.

(55) Andzelm, J.; Kölmel, C.; Klamt, A. Incorporation of solvent effects into density functional calculations of molecular energies and geometries. *J. Chem. Phys.* **1995**, 103, 9312–9320.

(56) Klamt, A.; Eckert, F.; Arlt, W. COSMO-RS: An Alternative to Simulation for Calculating Thermodynamic Properties of Liquid Mixtures. *Annu. Rev. Chem. Biomol. Eng.* **2010**, 1, 101–122.

(57) Schäfer, A.; Klamt, A.; Sattel, D.; Lohrenz, J. C. W.; Eckert, F. COSMO Implementation in TURBOMOLE: Extension of an efficient quantum chemical code towards liquid systems. *Phys. Chem. Chem. Phys.* **2000**, 2, 2187–2193.

(58) Stull, D. R. Vapor Pressure of Pure Substances. Organic and Inorganic Compounds. *Ind. Eng. Chem.* **1947**, 39, 517–540.

(59) Lin, S.-T.; Sandler, S. I. A Priori Phase Equilibrium Prediction from a Segment Contribution Solvation Model. *Ind. Eng. Chem. Res.* **2002**, 41, 899–913.

(60) Hiraga, Y.; Kato, A.; Sato, Y.; Smith, R. L. Densities at Pressures up to 200 MPa and Atmospheric Pressure Viscosities of Ionic Liquids 1-Ethyl-3-methylimidazolium Methylphosphate, 1-Ethyl-3-methylimidazolium Diethylphosphate, 1-Butyl-3-methylimidazolium Acetate, and 1-Butyl-3-methylimidazolium Bis(trifluoromethylsulfonyl)imide. *J. Chem. Eng. Data* **2015**, 60, 876–885.

(61) Shulgin, I.; Ruckenstein, E. Henry's Constant in Mixed Solvents from Binary Data. *Ind. Eng. Chem. Res.* **2002**, 41, 1689–1694.

(62) Song, D.; Chen, J. Density and Viscosity Data for Mixtures of Ionic Liquids with a Common Anion. *J. Chem. Eng. Data* **2014**, 59, 257–262.

(63) Mota-Martinez, M. T.; Brandl, P.; Hallett, J. P.; Mac Dowell, N. Challenges and opportunities for the utilisation of ionic liquids as solvents for CO₂ capture. *Mol. Syst. Des. Eng.* **2018**, 3, 560–571.